

## Elementary processes in plasma-surface interactions with emphasis on ions

P.C. Zalm

Philips Research Laboratories, 5600 JA Eindhoven - The Netherlands

Abstract Elementary processes occurring at solid surfaces immersed in low pressure plasmas are reviewed. In particular mechanisms leading to anisotropic or directional etching are discussed. The crucial role of ion bombardment is emphasized. First a brief summary of the interaction of (excited) neutrals, ions and electrons with targets is given. Next various aspects of sputter-etching with noble gas and reactive ions are surveyed. Finally it will be argued that synergistic effects, invoked by ion bombardment of a surface under simultaneous exposure to a reactive gas flux, are foremost important in explaining anisotropic plasma etching. It is shown that the role of the ions is not merely to stimulate the chemical reaction path but rather that the active gas flow chemically enhances the sputtering.

### INTRODUCTION

In these notes we will describe and discuss elementary processes occurring at solid surfaces immersed in low pressure plasmas. Many causes for an observed directionality in etching have been identified - crystal orientation preferentiality, ion-, electron- or photon- bombardment induced decomposition of polymerized adsorbates from the gas phase, etc. There is overwhelming evidence, however, that in the majority of cases where anisotropy was obtained in plasma etching ion bombardment of the surface to be etched played a crucial role. For this reason we will concentrate on the various phenomena accompanying ion bombardment and we try to explain their possible influence on directionality. For an extensive review the reader is referred to (ref. 1). The basic problem, which hampers the understanding of the interaction of a glow discharge with a solid, is the complexity of the whole system. Even in the simple case of a noble gas plasma environment we have to acknowledge the fact that both neutral atoms, a fraction of which may be in an excited state, ions, electrons and photons impinge on the surface simultaneously. Usually their fluxes and energies, if appropriate, are unknown and may vary with time. The use of gas mixtures, containing (fragments of) molecules, further complicates the situation.

An obvious way to circumvent, at least partially, the problems sketched above is to simulate selected process details by letting directed beams of atoms (molecules) and/or ions or electrons of well-controlled composition, flux and energy impinge on a surface in an otherwise UHV environment. Many authors have taken this phenomenological approach and with quite some success advanced our knowledge, as we will see below. With certainty, however, by far not all aspects of the mechanisms contributing to anisotropic plasma etching have been uncovered. Because of the very nature of such a limited simulation set-up synergistic effects and the influence of trace contaminants cannot simply be accounted for.

### THE INTERACTION OF LOW-ENERGY IONS, (EXCITED) NEUTRALS AND ELECTRONS WITH SOLID SURFACES

When ions emerging from a plasma can reach and bombard the target to be etched their energy is usually in the range of 30 eV to 3 keV. Furthermore we may assume that for most practical purposes the ions are incident perpendicularly to the surface. This assumption is only invalid if dimensions of surface topographical features (masks etc.) become comparable to the plasma sheath thick-

ness which is of the order of the Debye length,  $\lambda_D = (kT_e \epsilon_0 / n_e e^2)^{1/2} \sim 0.1-1$  mm. Because the electron mobility is much larger than the ion mobility, all surfaces in contact with a plasma will always be charged negatively. Therefore we shall consider only positive ions. Although it is acknowledged that the role of negative ions may be important in some RF etch plasmas (especially those based on e.g.  $\text{CCl}_4$ ,  $\text{SF}_6$  and  $\text{NF}_3$  gases, which have a high cross section for electron attachment), it has not been studied in much detail. Neutral atoms or molecules present in a plasma will essentially impinge upon a surface with thermal (sub-eV) energies. Neutrals excited in the gas phase will consequently only reach the surface in a metastable state, i.e. if they have sufficiently long lifetimes.

#### Neutralization, de-excitation and secondary electron emission

Much experimental and theoretical information about neutralization and de-excitation near metal surfaces was gathered by Hagstrum and co-workers and is reviewed in (ref. 2). As probably the same principles apply near semiconductor or isolator surfaces, we briefly summarize his treatment in Fig. 1.

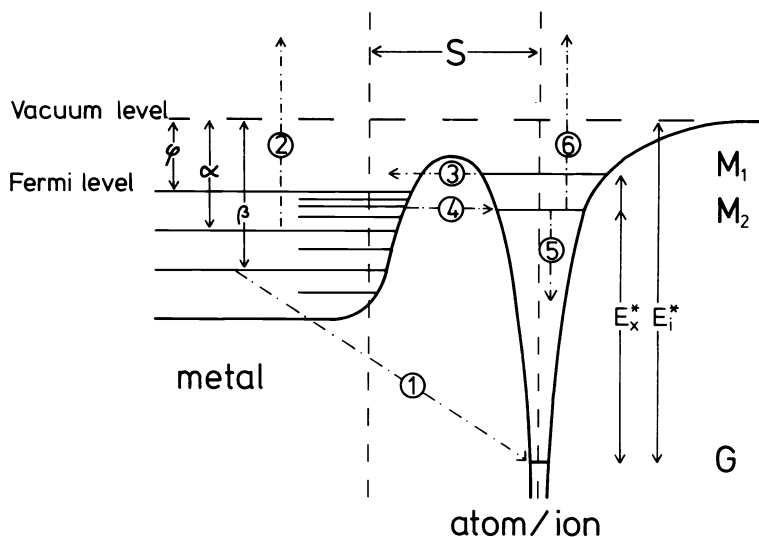


Fig. 1. Schematic diagram illustrating Auger neutralization or de-excitation of an ion or an excited atom, respectively, at a metal surface. Resonance neutralization and ionization processes are also indicated.  $\phi$  is the work function and  $E_i$  or  $E_x$  are the ionization or excitation energies, respectively ( $E_{i,x}$ ,  $E_{i,x}^*$  where  $E_{i,x}^*$  is the energy needed to ionize or excite an atom in free space).  $S$  is the distance of the particle from the surface.

Electronic transitions near ( $\sim 5\text{\AA}$ ) a metal surface are dominated by Auger or resonance type processes, which occur in about  $10^{-15}$  seconds. This is due to the fact that the probability for radiative processes is small owing to the long lifetime ( $\sim 10^{-8}$ s) for radiation relative to the time spent to travel the last few Ångströms to a surface for even a thermal particle. For the, relatively small, kinetic energies discussed here the ion neutralization probability is close to unity. Two parallel mechanisms are operative (see Fig. 1):

(i) An electron from a bound state ( $E_\beta$ ) in the metal tunnels into the ground state G of the ion (transition ①). The energy released by this transition is gained by a second electron in the metal ( $E_x$ ) which is excited (②). This process is known as Auger neutralization.

(ii) An electron from the metal may tunnel into a level of the same energy leaving a neutral but excited atom (transition ④), a process called resonance neutralization.

De-excitation of a metastable atom near a surface is also possible via two mechanisms:

(iii) The electron in the metastable level  $M_1$  of the atom may tunnel into an empty level in the metal leaving an ion (transition ③), a process named resonance ionization. Subsequent neutralization may proceed as in (i).

(iv) An electron from a bound level in the metal ( $E_\beta$ ) may tunnel into the ground state G of the metastable atom (①). The energy released in this

transition is consumed by ejecting the electron in the metastable state  $M_2$  of the atom (⑥). It is also possible that it is this electron which drops to the ground state (⑤), thereby ejecting an electron from the metal (2). These processes have been baptized Auger de-excitation. A consequence of the above-sketched schemes is that a secondary electron may be emitted from the surface if it has sufficient momentum perpendicular to that surface. The maximum kinetic energy of secondary electrons generated in such Auger processes is predicted to be  $E_i - 2\phi$  (ionization energy minus twice the work function of the solid) in excellent agreement with experimental observations (ref. 2). At low ion energies ( $\leq 1\text{keV}$ ), the total secondary electron yield is observed to be almost constant (ref. 2). A fairly accurate ( $\leq 25\%$ ) estimate of the electron yield in this so-called potential electron energy (PEE) regime - i.e. where the potential energy of the incoming ion dominates the secondary electron generation - is given by

$$\gamma_{\text{PEE}} \approx (0.8 E_i - 2\phi)/30. \quad (1)$$

At higher projectile energies, the excitation of weakly bound electrons in the solid through energy transferred from the penetrating particle - governed by the electronic stopping cross section - becomes an additional source for secondary electrons. This kinetic electron emission (KEE) mechanism is usually not dominant below 3keV. Contrary to PEE, many of the underlying processes in KEE are still not well understood and an adequate theoretical framework has not yet been provided (see e.g. ref. 3).

Although the secondary electrons are initially ejected with low energy (50eV) they may be accelerated over the plasma sheath away from the surface. Then these electrons can ionize atoms or molecules present in the reactor, thereby sustaining the gas discharge. This is especially important in RF plasmas driven with a frequency below the ion plasma frequency,  $f_i = (n_i e^2 / m_i \epsilon_0)^{1/2} / 2\pi$ . Only at the lowest gas pressures used in plasma etching ( $10^{-3}$  Torr) the secondary electrons will be able to impinge on the reactor walls, where ternary generations of electrons can be created.

#### (Excited) neutrals, electrons and photons impinging on a surface

Neutrals. We can be brief about the role of excited neutral (fragments of) molecules. Contrary to chemical reactions in the gas phase, which are known to be strongly affected by electronic excitation of the interacting species, their role is insignificant in plasma-wall interactions. The reason lies in the highly efficient Auger de-excitation processes "neutralizing" the molecules internal energy efficiently when it approaches the surface, as discussed before. All that can possibly be expected is that by ejection of electrons originally bound to target atoms decomposition and finally desorption of molecules present in the surface might take place. Given the relative unimportance of the electronic excitation energy we will from here onward only consider the behaviour of neutral atoms or molecules from the plasma in a general sense, ignoring internal energies of such particles.

Even if the atomic constituents of a molecule are highly reactive, given a certain surface composition, the molecule itself might not interact with the target. Dissociative chemisorption will only occur if the sum of the binding energies of each atomic constituent to the surface exceeds the molecular dissociation energy. For this reason several gases commonly used in plasma etching, as e.g.  $\text{CF}_4$ ,  $\text{C}_2\text{F}_6$ ,  $\text{CF}_3\text{Cl}$ ,  $\text{CF}_2\text{Cl}_2$ ,  $\text{CF}_3\text{H}$ ,  $\text{CCl}_4$ , are surprisingly inert on almost all surfaces. Their sticking probability is low and consequently the surface residence times of such molecules will be very small ( $\sim 10^{-6}\text{s}$ ). This does not necessarily imply, however, that the steady-state coverage may be neglected. For pressures of the order of  $10^{-2}$ -1 Torr - all but uncommon in plasma reactors - and high electron and ion densities in the plasma bombardment induced dissociation can still be important as we will see below.

In realistic plasmas not only complete molecules from the parent gas will be present but neutral molecular fragments and radicals abound. In the absence of strong evidence to the contrary, it should be assumed that radicals have reasonably large sticking coefficients and that they will react with the surface. [For example,  $\text{CF}_4$  does not stick on Si, but  $\text{CF}_x$  ( $x \leq 3$ ) does so with a probability of 0.08-0.75!]. Moreover, charged particle bombardment-induced modification of the surface too may alter the adsorption behaviour of molecules in a plasma environment. It should be noted that for molecular gases not all of the constituent atoms will necessarily always lead to a favourable reaction with the substrate atoms. Part or even all of the effects of the desired component may be counteracted by another.

If a gas as such does react spontaneously with the surface, several options exist. When the reaction leads immediately to volatile products, which desorb quickly, (rapid) isotropic etching results. Etch selectivity, i.e. the prefe-

rential removal of one type of atoms present on the surface to be etched, is likely to be high. Generally an adsorbed gas layer on top of the partly reacted surface will form. The depth to which this altered layer extends depends on the reactive gas flux, the removal rate by desorption and/or volatile product formation and the diffusion through this layer. Of course reactions may take place leading to stable compound formation (e.g. corrosion effects). [For example,  $\text{Cl}_2$  only chemisorbs dissociatively on the very surface of Si, whereas for  $\text{F}_2$  there is evidence that it not only reacts and etches directly but also that it penetrates to a depth of several monolayers.]

The chemical bonds formed will affect any sputtering action of the ions originating from the plasma. If the "structure" of the reacted surface layer is akin to a "Van der Waals" type solid, of more or less independent molecules, a sputtering yield enhancement results. When it resembles a "glassy" solid, with bond cross-linking, a reduction in sputtering yield may be observed. The former case is expected for monovalent reactive gas atoms, whereby upon reaction a single bond with a target atom replaces an atom-atom bond in the solid. Multivalent atoms from the reactive gas are more likely to form cross-links.

Electrons. Energetic electrons can excite electrons bound to target atoms. The creation of such so-called core holes may lead to a breaking of the chemical bond between atoms in or on the target surface. Thus, electron-bombardment-induced dissociation of adsorbed molecules might take place. For example, it is known that  $\text{Si}_3\text{N}_4$  and  $\text{SiO}_2$  do not react spontaneously with  $\text{XeF}_2$ . Simultaneous exposure to an electron beam, however, results in rapid etching, because of electron induced  $\text{F}_2$  dissociation (see ref. 4). [Note:  $\text{XeF}_2$  is a white solid with a high vapour pressure. When incident on a solid surface it immediately dissociates in Xe, which desorbs instantaneously, and  $\text{F}_2$ . The advantage of using  $\text{XeF}_2$  instead of  $\text{F}_2$  gas is that less precautions are required during e.g. transport.]

The possible bond-altering action of ion bombardment can also lead to target decomposition. For example, when  $\text{SiO}_2$  is bombarded with electrons it decomposes into silicon and, volatile, oxygen. In contrast, exposure of Si to an electron beam in the presence of oxygen causes the  $\text{O}_2$  to dissociate and promotes atomic oxygen diffusion into the bulk material thereby creating a surface oxide.

A survey of electron stimulated desorption on surfaces is given in (ref. 5). The cross sections for electron stimulated desorption on most surfaces are usually much smaller than for comparable gas phase processes involving electron induced dissociation and dissociative ionization. Nevertheless we believe gas-solid chemical reactions, which happen only in the presence of ion or electron bombardment, are widely occurring phenomena in a plasma environment.

Photons. (Multi-)photon absorption leads to atomic excitation. This in turn may invoke decomposition, enhance desorption or adsorption and adsorbate-adsorbate or adsorbate-adsorbent reactions. Laser-induced gas-surface interactions have been reviewed by Chuang (ref. 6). The photon fluxes needed to cause measurable changes are high (laser intensities of the order of  $0.1\text{-}1\text{ J/cm}^2$  are required in (repeated) pulse experiments!). Consequently it is considered unlikely that photons are important in plasma etching, except maybe on polymer targets, and we will not elaborate on this topic.

#### Phenomena accompanying ion penetration

Except for very light ions (e.g.  $\text{H}^+$  or  $\text{He}^+$ ), the slowing down mechanism upon penetration is dominated by kinetic energy loss of the ion in a series of binary collisions with target atoms initially at rest, in the energy range discussed here. This is called the elastic or nuclear stopping regime. In this process a number of fast recoils can be created which in turn set other target atoms in motion. A collision cascade develops and a continuously increasing number of progressively slower particles results until transferable energies become less than the displacement threshold ( $\approx 5\text{-}10\text{ eV}$ ). The time scale is of the order of  $10^{-13}\text{ s}$ . The collision cascade is finally damped by energy dissipation through e.g. phonon-assisted processes requiring typically about  $10^{-12}\text{ s}$  to set in and lasting about  $10^{-11}\text{-}10^{-10}\text{ s}$ . Until that time we have a locally "superheated" zone, of the order of the cascade volume around the ion's track, in which all atoms are agitated and move about with energies of the order of electron volts. Although the very concept of temperature is somewhat nebulous in this situation - an estimate would be  $T \sim 10^4\text{ K}$  -, enhanced diffusion, mixing and segregation of components present in or adsorbed onto the surface will occur.

At the lowest energies ( $\leq 100\text{ eV}$ ) the projected range, i.e. the penetration depth along the direction of incidence, is of the order of only  $10\text{ \AA}$ . The energies are too small to generate a collision cascade of displacements and effectively ion bombardment results in deposition. Even at room temperature epitax-

xial growth may be invoked in this way, because the deposited energy locally results in enhanced surface diffusion to favourable lattice sites. For the highest energies encountered in practical plasmas ( $\sim 3\text{keV}$ ) the projected range of the ions can be some  $100\text{\AA}$ , depending on the particular projectile/target combination. Radiation damage, inevitably accompanying ion bombardment, has been observed to extend to depths 3 - 10 times the ion range. As damage may affect electronic properties of the etched surfaces it could be desirable to remove such regions by an additional short plasma effluent or chemical wet etching step, even if such a process would be isotropic.

During the collision cascade development chemical bonds between target atoms are continuously broken. These are reestablished later, leading sometimes to the formation of new compounds with mixed-in adsorbed species or with the incident particle itself if it is chemically active. Thus, molecules volatile at the substrate temperature could form, a potential source for etching. Also ion-induced desorption may take place.

Finally sputtering, the ejection of target particles during ion bombardment, occurs. The latter process is considered extremely important in anisotropic plasma etching. Therefore an entire section will be devoted to this subject. Of course the impinging particles can reflect from the surface back into the plasma. For projectiles with a mass heavier than that of the target atoms and energies in excess of some  $100\text{eV}$  the reflection coefficient is usually fairly small. Only for very light ions ( $\text{H}^+$ ,  $\text{He}^+$ ) it can be substantial, ranging from over 50% to less than 25% in the energy range  $30\text{ eV}$ - $3\text{keV}$  on most target materials). Even if the reflection coefficient is small this does not necessarily imply that the trapping probability in the target is high, because subsequent ion bombardment is very effective in releasing previously implanted inert gas. Only if the implanted species can form strong bonds with the target atoms (either by chemical or dipole Van der Waals-type interactions) its retention may exceed the few percent level.

In the case of molecular projectiles incident on a surface the dissociation probability will be close to unity at energies above ca.  $100\text{eV}$ , because the energy transferred in the first collision is generally high compared to the internal binding energy of the molecule. The chemical reactivity of the constituent atoms is often much higher than that of the complete molecule. Thus molecular ion bombardment of surfaces can produce significant quantities of chemically reactive atoms and radicals both through bond-breaking in adsorbed molecules and by fragmentation of the incident projectile itself.

## SOME ASPECTS OF SPUTTERING

### Elemental targets

Theory. Perhaps the best founded, and with certainty the most widely applicable, theory of sputtering of elemental targets by atomic projectiles has been formulated by Sigmund (ref. 7). On the basis of linearized Boltzmann transport equation to describe the collision cascade in a semi-infinite and random medium he arrived at an expression for the backward sputtering yield at an ion energy  $E$  given by

$$Y(E) = \Lambda F_D(E, x=0). \quad (2)$$

Here  $F_D$  stands for the amount of energy deposited at the topmost atomic layers of the surface ( $x \approx 0$ ) in the form of target atomic motion.  $\Lambda$  is a material parameter encompassing the angle-, depth- and recoilenergy - averaged escape probability for target atoms set in motion in the cascade.  $F_D$  is linearly proportional to the (reduced) nuclear stopping cross section evaluated at the surface and  $\Lambda$  is inversely proportional to a surface escape barrier (usually taken to be equal to the sublimation energy).

The assumptions underlying eq. (2) are known to break down for a number of cases. For a full account of these the interested reader is referred to (ref. 7). In the energy regime discussed in these notes it suffices to know that the results of eq. (2) are invalid for low incident ion energies ( $\leq 100\text{eV}$ ) and for light ions, where the energy transferred is insufficient to allow for a proper collision cascade development. Several alternative approaches have been proposed to deal with these light ion and so-called threshold energy regimes, none of which are theoretically fully convincing although often satisfactory from a practical point of view.

For numerical evaluation eq. (2), in the case of perpendicular incidence, can be recast into the form

$$Y(E) = C_{pt} S_n(E/E_{pt}), \quad (3)$$

where  $C_{pt}$  and  $E_{pt}$  are characteristic constants depending on projectile and target parameters (viz. atomic number, mass and target atom sublimation energy  $U_0$  in [eV]). These are given by (ref. 8)

$$C_{pt} \approx (Z_p Z_t)^{5/6} / 3U_0 \quad (4)$$

applicable for  $1/16 \lesssim Z_t/Z_p \lesssim 5$ , which is roughly the region of validity of the theory itself, and the exact expression

$$E_{pt} = \frac{1}{32.5} \left(1 + \frac{M_p}{M_t}\right) Z_p Z_t (Z_p^{2/3} + Z_t^{2/3})^{3/2} \text{ [keV]}. \quad (5)$$

The reduced nuclear stopping cross section  $S_n(\epsilon)$  has been estimated reliably as (ref. 9)

$$S_n(\epsilon) = \frac{1}{2} \ln(1+\epsilon) / \left\{ \epsilon + \left(\frac{\epsilon}{383}\right)^{3/8} \right\}. \quad (6)$$

For incidence at an angle  $\vartheta$  with respect to the surface normal theory predicts a rise in yield proportional to  $\cos^{-n} \vartheta$ , with  $1 < n < 2$ , because the energy deposited in the outermost atomic layers ( $F_D$  in eq. (2)) increases. Experimentally such a dependence on  $\vartheta$  is observed to hold to about  $45^\circ$ , then the yield flattens off to a maximum at  $70^\circ \pm 10^\circ$  (of  $Y(\vartheta_{\max})/Y(0^\circ) \approx 3-10$ ) and rapidly drops to zero when  $\vartheta$  approaches  $90^\circ$  (glancing incidence), presumably because of particle reflection.

Comparison with experiment. Equations (3-6) have proven to be highly successful in predicting both the functional form of the energy dependence and the scaling with projectile or target parameters of the yield for ion energies exceeding a few hundred electron volts. Also the estimate of the absolute magnitude of the sputtering yield often agrees well with experiment. As an example the experimentally observed yields for noble gas ion bombardment of Si in the energy range of 0.2-400keV, divided by  $C_{pt}$ , are shown in Fig. 2 as a function of reduced energy  $\epsilon = E/E_{pt}$ . Indeed the  $S_n(\epsilon)$  curve is closely followed. However, for high target-to-projectile mass ratios (e.g.  $\text{Ne}^+$  on W) and also for heavy ions on heavy mass targets (i.e.  $M_p, M_t \approx 60$ ) the value of  $C_{pt}$  required to fit the experimental data has been observed to be lowered, sometimes by as much as 50%, relative to the theoretical value of eq. (4). Consequently the theory should be treated with some caution. A compilation of experimental sputtering yield data for atomic ion bombardment of elemental targets, along with a comparison with theory and some additional information is given in (ref.10).

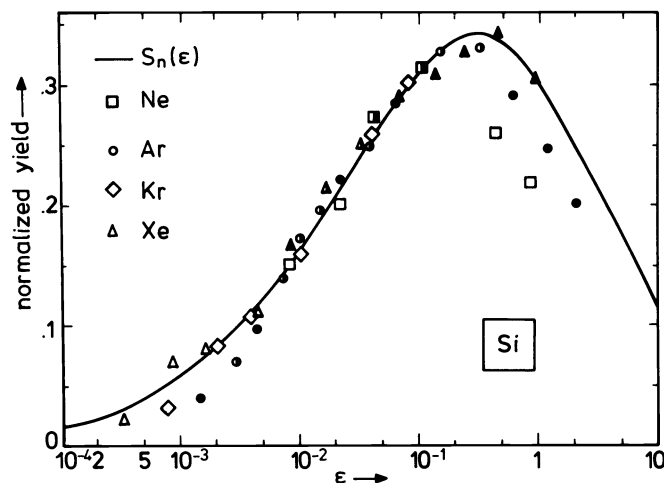


Fig. 2. Sputtering yield data for noble gas ion bombardment of silicon, at perpendicular incidence, as a function of reduced energy  $\epsilon$ . Yields are normalized to fit the predictions of the Sigmund model,  $Y(E) = CS_n(\epsilon)$ , eq.(3) in the text.

In order to circumvent the threshold problems in the low energy range ( $< 0.5\text{keV}$ ) discussed previously and to extend the use of eqs. (3-6) to this regime as well, the following empirical rule-of-thumb approach may be taken. Subtract from the yield calculated from eqs. (3-6) the value evaluated at the threshold energy  $E_{th}$ , which for practical purposes may be estimated as  $E_{th} \approx 8U_0$  for  $1/5 \lesssim Z_t/Z_p \lesssim 5$ . Strictly formally there is no theoretical foundation for such a forced ad hoc introduction of a threshold but it usually works well.

[As  $S_n(\epsilon)$  can be approximated by  $S_n(\epsilon) \approx 5/3 \epsilon^{1/2}$  at low energies ( $\lesssim 3 \text{ keV}$ ) a crude but simple estimate for the yield, at perpendicular incidence, including threshold effects can be extracted from eqs. (3-6) as (ref. 8)

$$Y(E) \approx 5 \cdot \sqrt{Z_t} (\sqrt{E} - 0.09 \sqrt{U_0}) / 3U_0$$

which, with  $E$  in [keV] but  $U_0$  in [eV], is valid to within 25% for  $1.5 \lesssim Z_t/Z_p \lesssim 5$ . This expression shows that the yield is not very dependent on projectile parameters other than incident energy.]

Sputtering with complex ions. Let us now turn to sputtering of elemental targets by complex molecular ions. As argued before, the molecule will fragment into its constituents upon impact on the surface at almost every energy ( $\approx 100$ eV). As a consequence the atoms will individually penetrate and involve a cascade. The total sputtering yield of the molecular ion may be taken as the sum of the yields of the individual constituents, as non-linear effects will be small in the energy range discussed here. The velocity of the atoms, originally forming the molecule, can be assumed equal to the original ion velocity - i.e.  $E_{\text{atom}} = m_{\text{atom}}/m_{\text{molecule}} \cdot E_{\text{ion}}$  - because the energy transferred in the first collision, although high compared to the molecular binding energy, is on average low with respect to the kinetic energy. Atomic sputtering yields may be taken from the compilation of experimental data (ref. 10), if available, or from the theoretical estimates, eqs. (3-6). The latter leads to the approximate result (ref. 8)

$$Y_{M \rightarrow T}(E) \approx C_{Mt} S_n(E/E_{MT}), \quad (7)$$

with

$$(C, E)_{Mt} = \sum_t (C, E)_{pjt} \quad (8)$$

where  $M$  stands for molecule and the sum is over all constituent atoms. Equations (7, 8) imply a "Sigmund"-like behaviour of the molecular ion yield. Thus, the characteristic constants determining magnitude and energy scaling of the sputtering yield for bombardment with a molecule must be taken as the sum of the respective characteristic constants of its constituent atoms. For a simple cluster ion of  $n$  identical atoms eqs. (7, 8) reduce to  $Y_n(E) = n \cdot Y_1(E/n)$ , a relation observed to be obeyed experimentally for dimer and trimer sputtering at moderate energies. Of course the same restrictions to the validity and use of eqs. (7, 8) apply as for eqs. (3-6), its theoretical "background". Experimental verification of eqs. (7, 8) is hampered by the fact that in practice molecular ions always contain chemically reactive atoms, for which the simple sputtering theory may not apply as will be discussed in the next subsection.

Compound targets. For compound targets current understanding of sputtering is still very incomplete and a satisfactory theoretical description is largely lacking. The theoretical and experimental situation is reviewed in (ref. 11). The major problems encountered in a description of the processes involved are preferential sputtering of one of the components and ion-induced segregation and diffusion. As a consequence the dynamics of the sputtering process must be modeled in order to understand the experimental situation. Time-dependent Monte-Carlo computer simulation codes have been developed to deal with this situation. Remarkable successes have been reported but, because of the particulars of a specific projectile/compound target combination, these have had little impact in the uncovering of underlying generalities. In spite of the considerable computational cost and modeling difficulties, related to the weighing of the various potentially competing phenomena, most future progress is expected to come from such simulations. In the mean time sound experimental data must be collected for particular, technologically urgent, cases.

#### Sputtering with reactive ions

Even in the absence of a possible chemical reaction between target and projectile atoms the trapping of the implanted species can result in a complicated behaviour of the sputtering yield, because of the alteration of the energy deposition, effects on chemical bonds, amorphization or even gas release. For example, for noble gas ion bombardment of Si the yield is found to increase with fluence to a steady-state maximum attained around  $10^{15}$  ions/cm<sup>2</sup> (ref. 12). Consequently the predictions of the sputtering theory discussed in the previous subsection do certainly not apply to bombardment with reactive ions, showing a high trapping probability, in an energy and dose regime where the sputtered depth extends to over the projected range of the ions. An increase in the yield, relative to the predictions of eqs. (3-6), may follow from weakening the bonds - lowering of  $U_0$ , the surface escape barrier -, enhancing the deposited energy density -  $F_D(E)$ , the kinetic energy transferred to target atom motion at the surface - and formation of volatile reaction products. In reverse, similar arguments can be put forward to expect a

yield decrease for specific projectile/target combinations. [The former situation probably exists in, for example, Si bombarded with  $F^+$  ions which might lead to  $SiF_4$  formation. Si bombardment with  $N^+$  or  $N_2^+$  ions results in silicon nitride formation, a material with a higher resistance to sputtering than Si itself.]

The most systematic investigations on Reactive Ion Beam Etching (RIBE) in relation to plasma processing have been carried out by groups at IBM (Coburn, Winters and co-workers, see e.g. (refs. 1,13)) and Hitachi (Miyake, Tachi and Tokuyama et. al., (ref. 14)), although many others have also contributed substantially. Almost all of these experiments were centered around ions of halogen - or halogen containing molecules incident on Si or its compounds. Often the sputtering yield obtained with such projectiles is related to the yield of comparable mass noble gas ions to show or deduce "chemical enhancement effects". This procedure has been subjected to critique, however, on the basis of the arguments leading to eqs. (7, 8) and general comments pertaining to the effects accompanying reactive ion implantation, as discussed before. Although the pioneering efforts by the IBM group are recognized, we will briefly summarize the general features observed in RIBE taking data from Hitachi as an example. The latter were obtained with mass-selected and energy-analyzed ion beams thus allowing for an easier interpretation. In fig. 3 the observed (ref. 14) energy dependences of the steady-state sputtering yields, of all possible projectiles resulting from ionization of  $CF_4$ , of Si bombarded at normal incidence are shown. As carbon ions are seen to be deposited onto or incorporated into the Si at all energies, also the curve for  $F^+$  on elemental C is included.

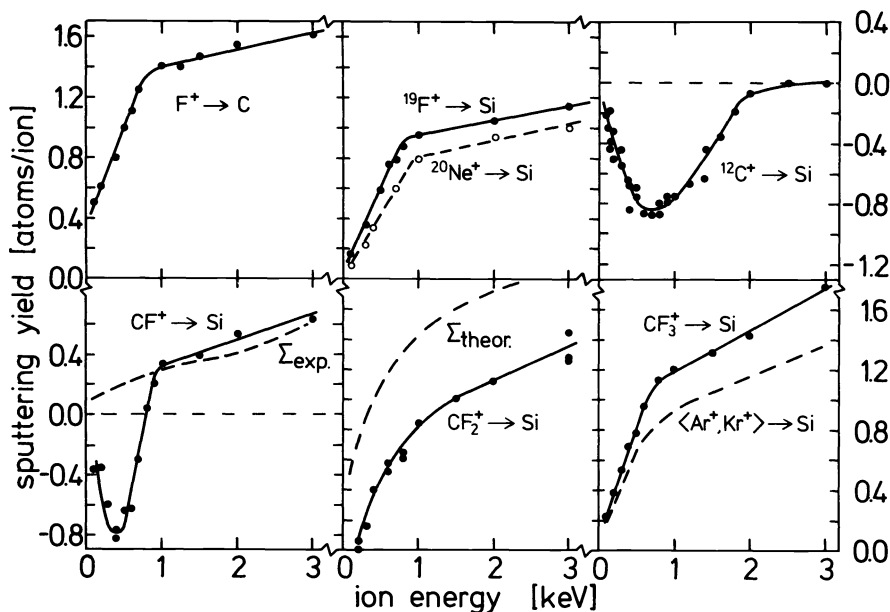


Fig. 3. Sputtering yield data for Si, bombarded with  $F^+$  and  $CF_n^+$  ions at perpendicular incidence, as a function of ion energy.  $\Sigma_{\text{theor}}$  is the prediction of eqs. (7,8),  $\Sigma_{\text{exp}}$  that of eq. (9). Details will be discussed in the text.

First consider the results for  $^{19}F^+$  or  $^{20}Ne^+$  on Si. The physical sputtering yield of both ions should be roughly equal according to eqs. (3-6). Thus, the observed yield increment of about 0.15 Si atoms/ion for  $F^+$  relative to  $Ne^+$  was attributed to  $SiF_4$  formation. As stated before, however, other arguments could apply - e.g. an increase in  $F_D(E)$  or a decrease in  $U_0$  due to  $F^+$  implantation, to keep in line with the language of eqs. (2-6) - and actually can explain the observations. Similar results were obtained in a comparison of Si sputtering yields for  $^{35}Cl^+$  and  $^{40}Ar^+$  ion bombardment, where also incorporation of Cl in the top atomic layers of the Si was observed. One must rightfully conclude that the chemical role of the reactive ion bombardment is not merely to stimulate the reaction path leading to volatile product formation. The trends observed for these and other reactive atomic ion elemental target combinations can be summarized in the following very crude rule-of-thumb estimates for the expected chemically induced yield enhancement or reduction, relative to the comparable mass noble gas ion result or the prediction of eqs.



(3-6):

i)  $\Delta Y_{\text{chem}} \approx a/b$ , if projectile P and target T can form a volatile compound  $T_aP_b$ . [Note:  $\approx$  to account for particle reflection and sputtering.]:

ii)  $\Delta Y_{\text{chem}} \sim -b/(a+b) \cdot Y_{\text{phys}}$ , if the product  $T_aP_b$  is involatile. [Note:  $\sim$  because it is only an order of magnitude estimate of the effect.]:

For all molecular (-fragment) ion bombardments studied to date it has been established that the observed sputtering yields lie below the theoretical predictions of eqs. (7, 8), the "fragmentation-into-it's-constituents" sum rule. In Fig. 3 the comparison is made for  $\text{CF}_2^+$  on Si ( $\approx$  the gives the estimate of eqs. (7, 8)). The reason is fairly simple: deposition or incorporation of one of the constituents is not accounted for by the theory! Consequently part of the other molecular constituents (F in this case) are needed to scavenge the deposit. Attempts have been made to account for this by using experimental elemental yield data in approach otherwise somewhat analogous to the one leading to eqs. (7, 8). In the case of  $\text{CF}_n^+$  on Si, such an experimental fragmentation sum rule would read (see e.g. ref. 15)

$$Y_{\text{CF}_n^+ \rightarrow \text{Si}}(E) = \left[ \frac{Y_{\text{C}^+ \rightarrow \text{Si}} \left( \frac{E}{1+n \cdot 19/12} \right)}{Y_{\text{F}^+ \rightarrow \text{C}} \left( \frac{E}{n+12/19} \right)} + n \right] \cdot Y_{\text{F}^+ \rightarrow \text{Si}} \left( \frac{E}{n+12/19} \right) \quad (9)$$

where experimental yield data at the appropriate energies have to be inserted. [Note that  $Y_{\text{C}^+ \rightarrow \text{Si}}$  has a negative sign!] In Fig. 3 the comparison is made for  $\text{CF}^+$  on Si ( $\sum_{\text{exp}}$  gives the estimate of eq. (9)), but similar observations pertain to  $\text{CF}_{2,3}^+$  on Si. The agreement is especially poor at lower energies. Again the reason is simple: carbon deposited onto or incorporated into silicon differs from elemental C (e.g. through carbide formation)! Thus the experimental values of  $Y_{\text{F}^+ \rightarrow \text{C}}$  are inapplicable in this case. Finally for  $\text{CF}_3^+$  on Si the yield curve in Fig. 3 is compared with the average of the (mutually almost identical) results for  $\text{Ar}^+$  and  $\text{Kr}^+$  on Si ( $M_{\text{Ar}}=40 < M_{\text{CF}_3}=69 < M_{\text{Kr}}=84$ ). We have already discussed why such a comparison is in fact quite meaningless. For compound targets the assessment of possible chemical enhancement effects upon the use of reactive (molecular) ions is further complicated by preferential sputtering, ion-induced segregation and diffusion. Yet another macroscopic problem arises because it has to be established whether or not all constituents in the compound can and/or will form volatile products. [For example, when  $\text{SiO}_2$  is bombarded with  $\text{CF}_n^+$ ,  $n \leq 3$  no carbon deposition takes place, presumably because of volatile CO formation. By the way, note that it has been known already for quite some time that for plasma-etching of Si in a  $\text{CF}_4$  discharge the results improved considerably if a few percent of  $\text{O}_2$  was added to the gas.] Again, it is impossible to give general rules for the expected sputtering yields of compound targets under reactive molecular ion bombardment. It appears, however, that observed reactive ion etch rate selectivities for an element and its compounds (e.g.  $Y_{\text{CF}_3^+ \rightarrow \text{Si}}/Y_{\text{CF}_3^+ \rightarrow \text{Si}_3\text{N}_4}$  or  $\text{SiO}_2$ ) are roughly of the same order of magnitude as those obtained under "real" plasma conditions with the same type of gas.

A major problem in RIBE simulations of plasma processes is that both for elemental and compound targets the absolute sputtering yield is usually an order of magnitude lower than the corresponding plasma etch rate. Consequently the basic principles underlying plasma etching have to be unraveled by yet another type of experiments, to be discussed in the last section.

#### SYNERGISTIC EFFECTS (CHEMICALLY ENHANCED/REDUCED SPUTTERING)

It has been known for a long time that the sputtering yield of metals bombarded with noble gas ions is considerably reduced if oxygen is introduced in the vacuum system as a contaminant gas. The reason for this is the formation of metal oxides, with a low sputtering yield, induced by ion beam mixing of adsorbed oxygen into the top atomic layers. Surprisingly, the reverse situation of a yield enhancement by simultaneous exposure to a reactive gas flux has begun to be explored only in the last decade. Pioneering work in this area was again carried out by the IBM group (Coburn and Winters et al., (ref. 4)). They showed that the etch rate of Si bombarded with  $\text{Ar}^+$  ions in the presence of  $\text{XeF}_2$  gas is enhanced by more than an order of magnitude when compared with the individual actions of either ions or gas separately. Fig. 4, taken from this work, has become a classic in the field. It was immediately recognized that these findings were very important for (anisotropic) plasma etching and that probably one of the fundamental processes had been uncovered. This initial success prompted many other research groups to start investigations along similar lines. Below we try to summarize the results, which allow for a qualitative understanding of synergistic effects of combined exposure of a surface to

ions and a reactive gas flux. Some general trends can now be given, but a quantitative description of etch rate enhancement or reduction awaits future developments.

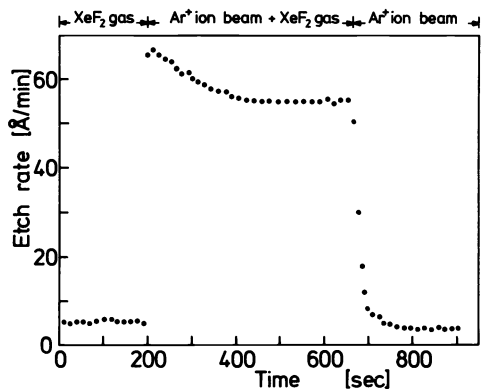


Fig. 4. The first experimental proof of ion-enhanced gas-surface chemistry: the Si(XeF<sub>2</sub>, 2·10<sup>15</sup> mol/s; Ar<sup>+</sup>, 450 eV, 2.5 μA) system.

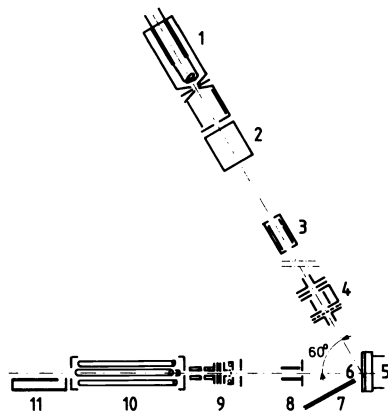


Fig. 5. Schematic, not to scale, view of the TOF apparatus. The symbols are discussed in the text.

Although obviously etch rates attract the direct attention, most of our understanding about the mechanisms in chemically assisted sputtering (or ion beam induced etching) stems from the study of the resultant reaction products. In particular the investigation of the emitted products' compositions and, perhaps even more significant, the kinetic energy distributions of the ejected particles as a function of ion energy and reactive gas-to-ion flux ratio has been foremost important. In Fig. 5 the experimental set-up is shown which was used to measure these quantities in the AMOLF-Philips collaboration (ref.16). A target (6), mounted on an oven (5) capable of heating the sample up to 1000K, is flooded with reactive gas from an inlet (7). Mass and energy selected ions from a source (1-4) impinge on the surface at an angle of 60°. Neutrals emitted from the target perpendicularly within a solid angle of 10<sup>-4</sup>sr pass a charged diaphragm (8) and are ionized (9) just in front of the entrance of a quadrupole mass spectrometer (10). Here the freshly formed ions are mass analysed and detected by an electron multiplier (11). Time-of-flight distributions can be measured by electronically modulating (3) the ion beam pseudo-randomly and coincident detection. Correlation techniques are used to unveil the particles' energy distributions. Only those signals, sufficiently above background, are detected which stem directly from neutrals ejected during ion bombardment. Corrections for velocity dependent ionization efficiency and flight time from source or to detector are applied in later off-line analysis. When silicon is exposed to a chlorine beam, no spontaneous reaction takes place. Above a target temperature of 300°C etching starts to become significant, the reaction product being SiCl<sub>4</sub>. At temperatures in excess of 800°C, removal of silicon as SiCl<sub>2</sub> dominates. It has been proven unambiguously, however, that when Si is bombarded with Ar<sup>+</sup> ions in the presence of a Cl<sub>2</sub> gas flux on the target - such systems will be denoted by Si(Cl<sub>2</sub>;Ar<sup>+</sup>) from here onward - Si, Cl, SiCl, SiCl<sub>2</sub> and (re-emitted previously implanted) Ar as such are ejected from the surface in roughly equal amounts under certain experimental conditions. These particular products themselves already cast serious doubts about the possibility that the role of the ions would be merely to stimulate the thermal reaction path by local heating of the surface upon impact. Observed "sputtering" yields for the Si(Cl<sub>2</sub>,Ar<sup>+</sup>) system exceed normal Ar<sup>+</sup> yields of Si by a factor of about 5, which constitutes yet another argument against such a process as a "superheated" cascade volume would have to small a surface area (<100Å<sup>2</sup>) and exist too short (<10<sup>-11</sup>s) to explain the observations. The strongest argument against a mere assisting role of the ions stems from the kinetic energy distributions of the reaction products. For a "thermal" behaviour the energy distribution would have a Maxwell-Boltzmann (MB) like shape, i.e. (see ref. 17)

$$\Phi_{MB}(E) \propto E \exp(-E/kT), \quad (10)$$

with T either the substrate temperature, T<sub>S</sub>, or the temperature of the superheated zone, T<sub>LTE</sub>, in a Local Thermal Equilibrium type approximation. In any case T should be the same for all reaction products ejected. In a normal physical sputtering or collision cascade (C-C) model the kinetic energy distribution, for elements emitted perpendicularly to the surface, is given by (see e.g. ref. 17 for a general introduction)

$$\Phi_{C-C}(E) \propto E/(E+U_0)^3, \quad (11)$$

where  $U_0$  is the surface escape barrier for the particular product emitted, which is usually identified with the particle's binding energy inside the solid. [Note that for ejected (fragments of) molecules eq. (11) is only valid up to its dissociation energy,  $E_d$ . The asymptotic roll-off at high ejection energies ( $E \gg E_d$ ) becomes  $E^{-n/4}$ , where  $n$  is the number of atomic constituents.]

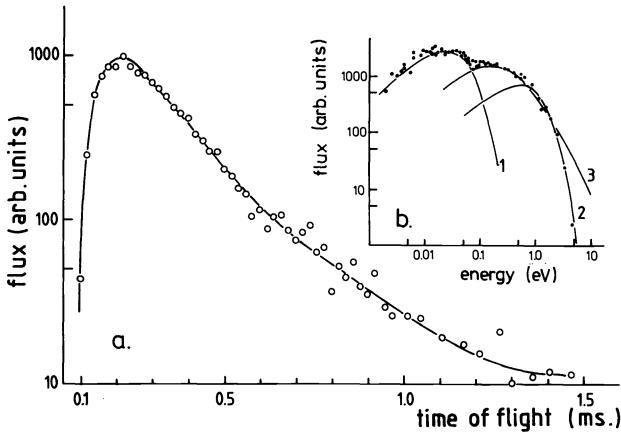


Fig. 6

a) Time-of-flight spectrum of SiCl obtained by bombarding Si at 300°C with 3 keV  $\text{Ar}^+$  ions (flux approx.  $5 \times 10^{14}/\text{cm}^2\text{s}$ ) under simultaneous exposure to a  $\text{Cl}_2$  gas flux of about  $5 \times 10^{16}/\text{cm}^2\text{s}$ .

b) Insert. Corresponding energy distribution curve. The fitted substrate temperature Maxwell-Boltzmann distribution (1) as well as a local thermal equilibrium contribution (2), fitted to the high energy tail, and a collision cascade contribution (3) are indicated.

The experimentally observed kinetic energy distributions of products ejected in the  $\text{Si}(\text{Cl}_2;\text{Ar}^+)$  or  $\text{Si}(\text{XeF}_2;\text{Ar}^+)$  systems are more complicated than eqs. (10) or (11) suggest. In general, however, the major part of a spectrum follows the predicted collision cascade behaviour of eq. (11). An example is given in Fig. 6, which shows both the raw time-of-flight data and the extracted energy spectrum for SiCl from  $\text{Si}(\text{Cl}_2, 5 \times 10^{14}/\text{cm}^2\text{s}; \text{Ar}^+, 3 \text{ keV}, 5 \times 10^{16}/\text{cm}^2\text{s})$ . A low energy MB contribution at  $T_s$  is sometimes observed (curve 1), which is believed to be due to molecules released from the bulk by desorption out of the void tunnel along the ion track. This contribution, if present at all, is always less than 20% of the total. A high temperature LTE-type MB contribution (2) can at best explain only the medium or the high energy part of only a single individual product's spectrum and certainly not the spectra for all products simultaneously with one  $T_{\text{LTE}}$ . fitting the kinetic energy distributions with the CC predictions (see e.g. curve 3 in Fig. 6 but remember the note following eq. (11)) gives good agreement. The extracted "binding energies"  $U_0$  for all individual products emitted, under the conditions valid for Fig. 6, are:  $U_0(\text{Si}) \approx 4 \text{ eV}$ , slightly below the sublimation energy of silicon;  $U_0(\text{Cl}) \approx 2 \text{ eV}$ , typical for Si-Cl bond energies;  $U_0(\text{SiCl}_{1,2}) \approx 0.4 \text{ eV}$ , indicative for the interaction of a highly polarizable molecule with a solid;  $U_0(\text{Ar}) \approx 0.05 \text{ eV}$ , typical for the Van der Waals binding energies of a noble gas atom in a solid. These observations reveal a very important aspect of the role of the bombarding ions. Obviously mixing of adsorbed species into the topmost atomic layers takes place. The mixed-in reactive species will form bonds with the target atoms, thereby "weakening the solid. In turn this enhances the sputtering yield, cf. eqs. (3.6). [SiCl<sub>2</sub> molecules with their observed low binding energies of only 0.4 eV could never have resided on the surface: they would simply desorb instantaneously! For the  $\text{Si}(\text{Cl}_2;\text{Ar}^+)$  system it has been established independently (ref. 18) that Cl exists inside the outermost atomic layers. The reduction of  $U_0(\text{Si})$  in the  $\text{Si}(\text{Cl}_2;\text{Ar}^+)$  system relative to the sublimation energy of Si is evidence for the weakening-by-mixing mechanism.] Both mixing efficiency and sputtering yield increase with the deposited energy (as target atom motion) distribution function  $F_D(E)$ , cf. eq. (2), which in turn increases with energy roughly  $E^{-n/4}$  in the range considered here. Many different regimes exist depending on whether the rate of mixing is faster, slower or comparable to the removal rate. The dependence on ion beam angle of incidence will in general differ from the one observed in standard sputtering situations as discussed following eq. (6), because of the complex interplay of mixing and etching. Substrate temperature influences the steady state adsorption and consequently also mixing. The reactive gas-to-ion flux ratio will largely determine the particular situation one will be in, with the exception of rather special cases where the chemistry is radically different from the usual situation. [For example, in  $\text{Si}(\text{F}_2$  or  $\text{XeF}_2$ ; noble gas ion) mixing of F into the Si is spontaneous, even on the absence of ions, because of fluorine diffusion. For  $\text{Si}(\text{SF}_6$ ; noble gas ion) at room temperature only normal physical sputtering occurs because the surface coverage with  $\text{SF}_6$  is negligible as it will not stick. At -200°C a thick condensed  $\text{SF}_6$  layer will form and we have essentially sputtering of frozen  $\text{CF}_6$  gas!]

More and more investigations on ion-assisted gas-surface interactions are being reported. Diamond has recently been etched successfully in the

C(NO<sub>2</sub>;Xe<sup>+</sup>,2keV,1mA/cm<sup>2</sup>) system (ref. 19) and etching of indiumphosphide in the InP(Cl<sub>2</sub>;Ar<sup>+</sup>) system has been reported (ref. 20), but many more examples could be mentioned. We have concentrated on Si(Cl<sub>2</sub>;Ar<sup>+</sup>) only because it is probably the best (i.e. most extensively) studied system to date. The regularities observed for this model system, however, seem to extend their validity to almost all others, be it that process details may differ considerably thereby seemingly refuting general conclusions. Fortunately it appears that there is no evidence contradicting the occurrence of the basic processes outlined in these pages, although the relative importance of the various (complementary) processes may differ from case to case.

## CONCLUSIONS

In these notes we have discussed elementary processes occurring at solid surfaces immersed in low pressure plasmas. The importance of energetic particle impingement onto targets was stressed. In particular the role of synergistic effects, by simultaneous exposure of a surface to a reactive gas beam and energetic particle bombardment, for plasma etching has been emphasized. Although it is easy to comprehend the physics underlying the observed phenomena, limited predictive power emerges from the remarks and conclusions presented in these pages because they are not readily transferable to processes taking place under realistic plasma conditions. Our intention was only to present some broad views about what might be going on and make you aware that there are no obvious conclusions which can be drawn in advance, when starting with a novel plasma scheme. [Some examples: (i) The presence of ions not necessarily implies loss of etch selectivity. Si bombarded ions in the presence of F<sub>2</sub> gas etches faster than with only either one, whereas F<sub>2</sub> inhibits Al sputtering by ions. (ii) The presence of ions does enhance directionality, but etch anisotropy may nevertheless be small because of other rapidly etching constituents in the plasma.]

The influence of plasmas on polymers (resists, masks etc.), although recognized as an important topic, has been carefully avoided in these notes. The matter is highly complicated and by far not as well established and investigated as simple elemental or compound solids.

Finally, one remark seems appropriate. It must be acknowledged that no justice could be done to many excellent contributions in the field of plasma-wall interactions. The list of references is far from complete and only intended to serve as an entrée in the literature.

## REFERENCES

1. H.F. Winters, Topics in Current Chemistry **94**, 69 (1980).
2. H.D. Hagstrum, Inelastic Ion-Surface Collisions, p.1, Wiley, New York (1977).
3. P.C. Zalm and L.J. Beckers, Philips J. Res. **39**, 61 (1984).
4. J.W. Coburn and H.F. Winters, J. Appl. Phys. **50**, 3189 (1979); J. Vac. Sci. Technol. **16**, 391 (1979); B1, 469/927 (1983); Surf. Sci. **103**, 177 (1981); 123, 427 (1983).
5. M. Knotek, Repts. Progr. Phys. **47**, 1499 (1984).
6. T.J. Chuang, Surf. Sci. Repts. **3**, 1 (1983).
7. P. Sigmund, Sputtering by Particle Bombardment I, p.9, Springer, Berlin, (1981).
8. P.C. Zalm and L.J. Beckers, J. Appl. Phys. **54**, 2660 (1983); **56**, 220 (1984); Rad. Eff. Lett. **86**, 29 (1983); J. Vac. Sci. Technol. **B2**, 151 (1984).
9. W.D. Wilson, L.G. Haggmark and J.P. Biersack, Phys. Rev. **B15**, 2458 (1977).
10. H.H. Andersen and H.L. Bay, Sputtering by Particle Bombardment I, p.145, Springer, Berlin, (1981).
11. G. Betz and G.K. Wehner, Sputtering by Particle Bombardment II, p. 1, Springer, Berlin, (1983).
12. J. Kirschner and H.W. Etzkorn, Appl. Phys. **A29**, 133 (1982).
13. J.W. Coburn and H.F. Winters et al., J. Appl. Phys. **48**, 3532/4973 (1977).
14. K. Miyake, S. Tachi and T. Tokuyama, Jap. J. Appl. Phys. **20**, L411 (1981); **21**, 141 (1982); J. Appl. Phys. **53**, 3214 (1982).
15. C. Steinbrüchel, J. Vac. Sci. Technol. **B2**, 58 (1984).
16. A.W. Kolfschoten, F.H.M. Sanders, J. Dieleman, P.C. Zalm, R.A. Haring and A.E. de Vries et al., Appl. Phys. Lett. **41**, 171 (1982); J. Appl. Phys. **55**, 3813 (1984); J. Vac. Sci. Technol. **A2**, 487 (1984); Nucl. Instr. Meth. **B7/8**, 809 (1985); to be published.
17. R. Kelly, Surf. Sci. **90**, 280 (1979); Rad. Eff. **80**, 167 (1983).
18. T. Mizutani, C.J. Dale, W.K. Chu and T.M. Mayer, Nucl. Instr. Meth. **B7/8**, 825 (1985).
19. N.N. Efremow, M.W. Geis, D.C. Flanders, G.A. Lincoln and N.P. Economou, J. Vac. Sci. Technol. **B3**, 416 (1985).
20. N.L. DeMeo, J.P. Donnelly, F.J. O'Donnell, M.W. Geis and K.J. O'Connor, Nucl. Instr. Meth. **B7/8**, 814 (1985).